

Radar Bias Error Removal Algorithm for a Multiple-Site System

A. GRINDLAY

*Radar Analysis Branch
Radar Division*

April 13, 1981



NAVAL RESEARCH LABORATORY
Washington, D.C.

Approved for public release; distribution unlimited.

REPORT DOCUMENTATION PAGE		READ INSTRUCTIONS BEFORE COMPLETING FORM
1. REPORT NUMBER NRL Report 8467	2. GOVT ACCESSION NO.	3. RECIPIENT'S CATALOG NUMBER
4. TITLE (and Subtitle) RADAR BIAS ERROR REMOVAL ALGORITHM FOR A MULTIPLE-SITE SYSTEM		5. TYPE OF REPORT & PERIOD COVERED Interim report on a continuing NRL problem.
		6. PERFORMING ORG. REPORT NUMBER
7. AUTHOR(s) A. Grindlay		8. CONTRACT OR GRANT NUMBER(s)
9. PERFORMING ORGANIZATION NAME AND ADDRESS Naval Research Laboratory Washington, D.C. 20375		10. PROGRAM ELEMENT, PROJECT, TASK AREA & WORK UNIT NUMBERS NRL Problem 53-0627-00 62712N, SF12133401
11. CONTROLLING OFFICE NAME AND ADDRESS Department of the Navy Naval Sea Systems Command (NSEA-61R2) Washington, D.C. 20362		12. REPORT DATE April 13, 1981
		13. NUMBER OF PAGES 14
14. MONITORING AGENCY NAME & ADDRESS (if different from Controlling Office)		15. SECURITY CLASS. (of this report) UNCLASSIFIED
		15a. DECLASSIFICATION/DOWNGRADING SCHEDULE
16. DISTRIBUTION STATEMENT (of this Report) Approved for public release; distribution unlimited.		
17. DISTRIBUTION STATEMENT (of the abstract entered in Block 20, if different from Report)		
18. SUPPLEMENTARY NOTES		
19. KEY WORDS (Continue on reverse side if necessary and identify by block number) Bias errors Multiple site integration		
20. ABSTRACT (Continue on reverse side if necessary and identify by block number) An algorithm has been developed to estimate the bias errors in the measurements made at two separate radar sites. This was accomplished by considering the measurements made on several common tracks and by using the difference vector between the measurements as the input to a Kalman filter to produce smoothed bias errors in range, azimuth, and elevation for each site. For purposes of this study the location of each site was assumed to be known exactly.		



CONTENTS

1.0 INTRODUCTION	1
2.0 ALGORITHM DEVELOPMENT	1
3.0 RESULTS WITH SIMULATED DATA	3
4.0 RESULTS WITH REAL DATA	6
5.0 SUMMARY	8
6.0 ACKNOWLEDGMENTS	9
7.0 REFERENCES	9
APPENDIX	11



RADAR BIAS ERROR REMOVAL ALGORITHM FOR A MULTIPLE-SITE SYSTEM

1.0 INTRODUCTION

Recent investigations as to the feasibility of operating a multiple platform sensor integration system [1-3] have led to the problem of removing bias errors from transmitted data. Bias errors are those errors, inherent to each sensor system, which may have been introduced during the construction or alignment of the sensor or are present as a result of equipment failures. With three-dimensional radar systems the problem reduces to one of detecting the bias errors that may be present in the range azimuth and elevation measurements made by each of the radars within the network of participating platforms. The solution of this problem is fundamental to the successful operation of a multiple platform sensor integration network. If bias errors cannot be detected and their effect reduced to a tolerable level, the advantages to be gained from the exchange of information between platforms cannot be realized. As a first step in this direction an algorithm has been developed for the special case of two fixed radars with known locations. The algorithm has been tested with simulated data and with real measurements. The measurements were made on targets of opportunity by two radars located at NRL's Chesapeake Bay Detachment (CBD) and at the Applied Physics Laboratory (APL) of the Johns Hopkins University. The results are presented in Sec. 3.0 and 4.0. With minor adjustments to the algorithm, the same basic concept should be applicable to the moving platform case.

2.0 ALGORITHM DEVELOPMENT

The problem which was taken under consideration is described as follows: Given the time history of measurements (range, azimuth, and elevation) on several distributed targets as measured by two separate radars, determine the measurement biases for each radar under the assumption that the exact location (latitude, longitude, and elevation) of each radar on International Geoid is known.

A two-dimensional representation of the geometry of the problem is shown in Fig. 1. Coordinate systems are established at each site with the x -axis pointing due east, the y -axis pointing to true north, and the z -axis (not shown) pointing outward along a line joining the site and the Earth's center. Azimuth is measured clockwise from the y -axis, elevation from the horizontal plane containing the x and y axes, and range is the Euclidian distance between the site and the target. The range, azimuth, and elevation measurements can readily be transformed to the local rectangular coordinate systems at each site. This allows us to express the measured position vector of a target with respect to Site 1 as

$$X_1 = \bar{X}_1 + A_1 B_1 + A_1 N_1, \quad (1)$$

where

$$X_1 = \begin{bmatrix} x_1 \\ y_1 \\ z_1 \end{bmatrix}, \quad \bar{X}_1 = \begin{bmatrix} \bar{x}_1 \\ \bar{y}_1 \\ \bar{z}_1 \end{bmatrix}, \quad B_1 = \begin{bmatrix} \Delta_{r1} \\ \Delta_{\alpha 1} \\ \Delta_{\eta 1} \end{bmatrix}, \quad N_1 = \begin{bmatrix} N_{r1} \\ N_{\alpha 1} \\ N_{\eta 1} \end{bmatrix},$$

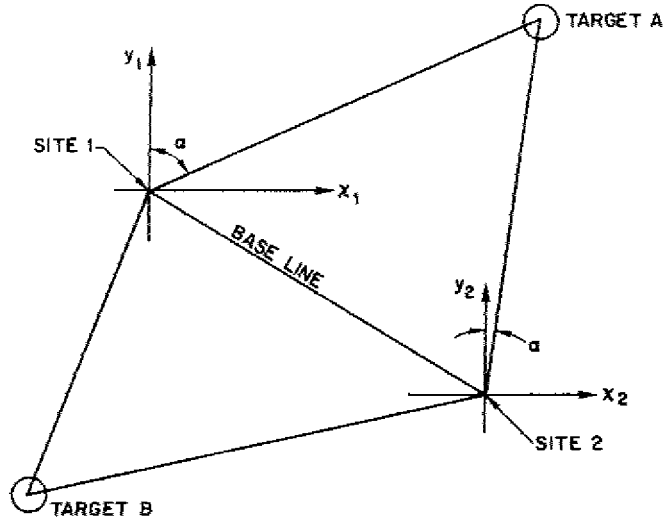


Fig. 1 — Geometric representation of the problem

$$A_1 = \begin{bmatrix} \partial x_1 / \partial r_1 & \partial x_1 / \partial \alpha_1 & \partial x_1 / \partial \eta_1 \\ \partial y_1 / \partial r_1 & \partial y_1 / \partial \alpha_1 & \partial y_1 / \partial \eta_1 \\ \partial z_1 / \partial r_1 & \partial z_1 / \partial \alpha_1 & \partial z_1 / \partial \eta_1 \end{bmatrix}, \quad \begin{array}{l} r = \text{range, } \alpha = \text{azimuth} \\ \text{and } \eta = \text{elevation} \end{array}$$

with X_1 being the position vector of the target at some instant, \bar{X}_1 being the mean or true position at the same time, B_1 being the vector of bias errors, N_1 being zero mean noise on the measurements, and A_1 being a matrix of partial derivatives which are derived in the appendix. Equation (1) is in effect a truncated Taylor's series expanded about the target's true position. The measurements made at Site 2 can also be converted to the local rectangular coordinate system at Site 2 and transformed to the local rectangular coordinate system at Site 1. This enables us to express the position vector of the target as measured by Site 2 with respect to Site 1 as

$$X_2 = \bar{X}_2 + A_2 B_2 + A_2 N_2, \quad (2)$$

where $A_2 = \begin{bmatrix} \partial x_2 / \partial r_2 & \partial x_2 / \partial \alpha_2 & \partial x_2 / \partial \eta_2 \\ \partial y_2 / \partial r_2 & \partial y_2 / \partial \alpha_2 & \partial y_2 / \partial \eta_2 \\ \partial z_2 / \partial r_2 & \partial z_2 / \partial \alpha_2 & \partial z_2 / \partial \eta_2 \end{bmatrix},$

i.e., A_2 is the matrix of partial derivatives representing the rate of change of Site 1 rectangular coordinates due to changes in the measurements made at Site 2, B_2 is the vector of bias errors at Site 2, and N_2 is the vector with elements that represent the noise on the elements made at Site 2. If the measurements at Sites 1 and 2 are not made at the same instant, it is possible to predict a "measured" position at some common time and still have Eqs. (1) and (2) hold provided the partial derivatives are not changing significantly. When Eqs. (1) and (2) represent coincident measurements, $\bar{X}_1 = \bar{X}_2$ and it is possible to subtract Eq. (2) from Eq. (1) to yield

$$\Delta X = A_1 B_1 - A_2 B_2 + A_1 N_1 - A_2 N_2, \quad (3)$$

where $\{\Delta X\}$ represents the Euclidean distance between the two measurements. Equation (3) can also be expressed in the form

$$\Delta X = M \cdot B + N, \quad (4)$$

where $M = \begin{bmatrix} A_1 & -A_2 \end{bmatrix}$, $B = \begin{bmatrix} B_1 \\ \dots \\ B_2 \end{bmatrix}$, and $N = M \cdot \begin{bmatrix} N_1 \\ \dots \\ N_2 \end{bmatrix}$.

Equation (4) is now in the form of the observation equation for linear estimation. In this case the ΔX vector represents the measurements and the B vector of bias errors is the state vector. The state equation is given by

$$B(t+1) = I \cdot B(t). \quad (5)$$

Note that the state transition matrix is the identity matrix since the bias errors are assumed to be constant over the period of interest; i.e., the bias errors at some future state ($t+1$) are equal to the bias errors at the current state (t).

With this formulation (Eqs. (4) and (5)) it is possible to predict the bias errors using the Kalman filter algorithm. (See Ref. 4 for a typical application.) The six steps involved in the recursive algorithm are as follows:

Step 1. Calculate one-step prediction,

$$\hat{B}(t|t-1) = \hat{B}(t-1|t-1), \quad (6)$$

where the circumflex signifies an estimate, $\hat{B}(t|t-1)$ indicates the predicted bias, and $\hat{B}(t-1|t-1)$ indicates the smoothed bias of $B(t)$.

Step 2. Calculate the predicted covariance matrix $P(t|t-1)$ from the smoothed covariance $P(t-1|t-1)$ by

$$P(t|t-1) = P(t-1|t-1). \quad (7)$$

(Note that for this case the predicted covariance matrix and state vectors are assigned the values determined at the previous time step since the state transition matrix is the identity matrix.)

Step 3. Calculate the predicted observation $\hat{\Delta X}(t|t-1)$ by

$$\hat{\Delta X}(t|t-1) = M(t) \hat{B}(t|t-1), \quad (8)$$

where $M(t)$ is the measurement matrix M at the t th sample.

Step 4. Calculate the filter gain $w(t)$ using

$$w(t) = P(t|t-1) \tilde{M}(t) [M(t)P(t|t-1) \tilde{M}(t) + R(t)]^{-1}, \quad (9)$$

where the tilde indicates the transpose of a matrix and $R(t)$ is the covariance matrix of the noise.

Step 5. Calculate a new smoothed estimate

$$\hat{B}(t|t) = \hat{B}(t|t-1) + w(t) [\Delta X(t) - \hat{\Delta X}(t|t-1)], \quad (10)$$

where $\Delta X(t)$ is the measurement vector ΔX in Eq. 4 at the t th sample.

Step 6. Calculate a new covariance matrix

$$P(t|t) = [I - w(t) \cdot M(t)] P(t|t-1). \quad (11)$$

The measurement covariance matrix R is the covariance of N ; i.e.,

$$R = \text{cov}(N) = E \{ (A_1 \cdot N_1 - A_2 \cdot N_2) (A_1 \cdot N_1 - A_2 \cdot N_2)^T \}. \quad (12)$$

Under the assumption that the partial derivatives are changing slowly in the neighborhood of the target location, a good approximation of the covariance is

$$\text{cov}(N) = A_1(\overline{N_1 N_1^T})A_1^T + A_2(\overline{N_2 N_2^T})A_2^T \quad (13)$$

or alternatively

$$\text{cov}(N) = M(\overline{N \cdot N^T})M^T \quad (14)$$

It should be noted that in calculating the partial derivatives which are the elements of the M matrix, that the smoothed estimate of the bias errors is applied to the measured range, azimuth, and elevation to provide an evaluation closer to the true position of the target. The matrix $(N \cdot N^T)$ is a diagonalized matrix with the diagonal elements being equal to the variances in the measurements of each radar. These were assigned typical values for the radars that were used.

3.0 RESULTS WITH SIMULATED DATA

To check out the algorithm described in Sec. 2.0, a set of simulated tracking data was developed. Stationary targets were chosen to simplify the process. When moving targets are being tracked further complications arise. Since the measurements at both sites are not made simultaneously a prediction of one of the measured positions, to some common time, must be made. This prediction process is not required for stationary targets since the predicted position is the current position.

Six stationary points in space, surrounding the locations of the two sites (NRL's Chesapeake Bay Detachment and APL) were selected as targets. The locations of the targets and their respective latitudes and longitudes are shown in Fig. 2. All of the target points were assumed to be at an altitude of 10,000 m.

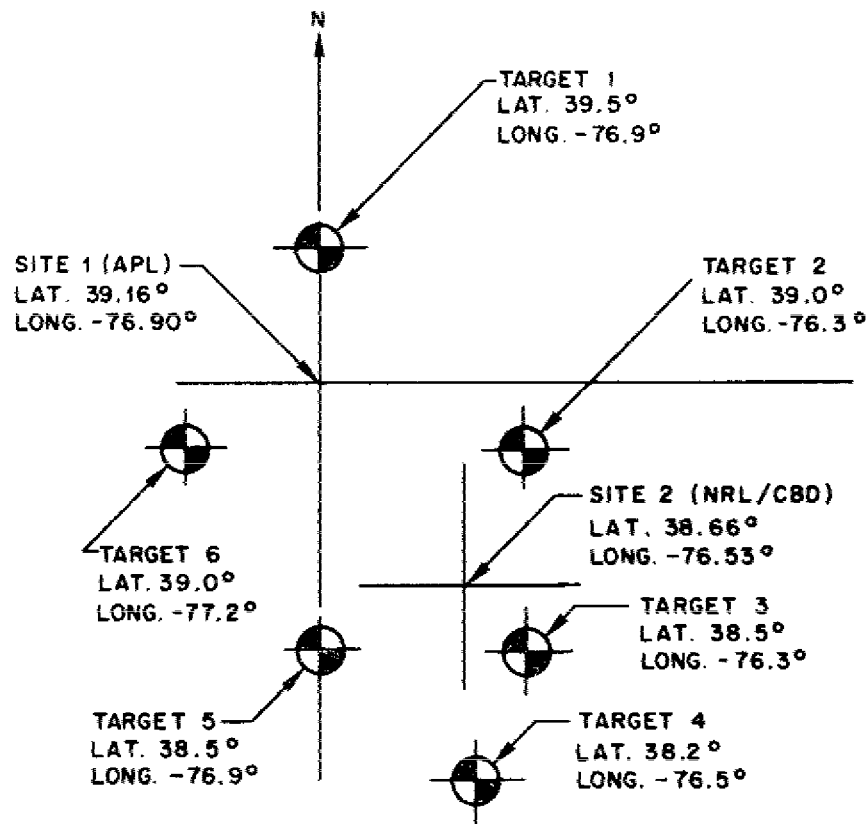


Fig. 2 — Location of simulated targets

Measurement data were generated by selecting samples from a Gaussian distribution derived from a random number generator and by adding these samples to respective range, azimuth, and elevation coordinates at each site. Bias errors that would adequately test the algorithm were also added to the measurements at this point. This resulted in a set of simulated measurements (range, azimuth, and elevation) for each of the six targets as measured by both sites. The difference in the location of each target as measured by both sites was used as the input to the Kalman filter. The process of simulating a detection of all the targets by each site was repeated 50 times or equivalently 50 rotations of each radar.

The computer-generated bias errors as predicted by the algorithm are presented graphically in Figs. 3 and 4. They show the estimated bias error as a function of time; the time units being the number of scans completed by both radars from the initial time until the time at which the estimate is made. Several cases with a wide range of induced bias errors were simulated. The case which is illustrated in Figs. 3 and 4 had the following induced errors at the APL site:

range bias error = 2 n.mi

azimuth bias error = -3°

elevation bias error = 3° ;

and at the NRL site:

range bias error = -2 n.mi

azimuth bias error = 3°

elevation bias error = -3° .

The results presented in Figs. 3 and 4 are from a single case, i.e., both sets of bias errors were induced simultaneously. As can be seen from the figures, a reasonably good estimate of the bias errors can be obtained after only three or four scans of the radars. The curve that represents the estimate of the elevation bias is not as smooth as the other curves. This is due to the value assumed for the variance in the measurement. The standard deviations assumed for the range, azimuth, and elevation measurements were 400 m, 0.5° , and 1.0° , respectively.

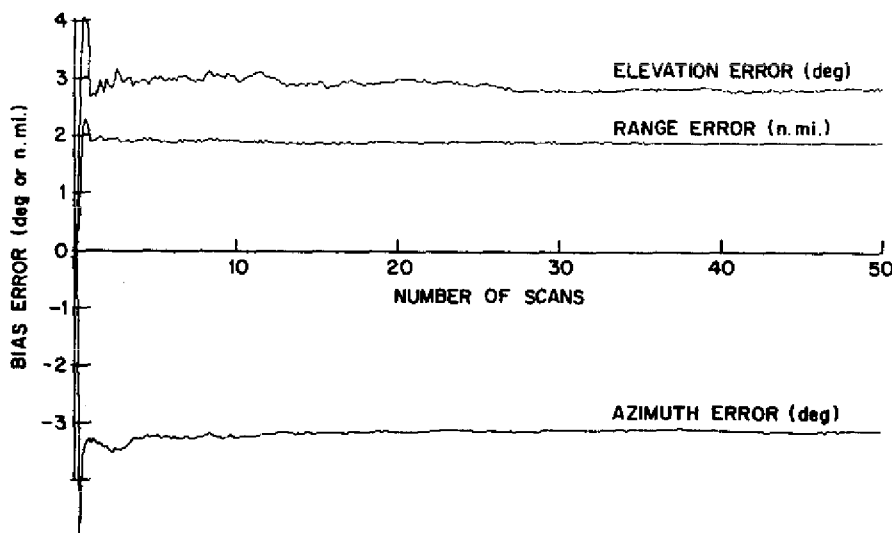


Fig. 3 — Estimate of induced bias errors in APL radar

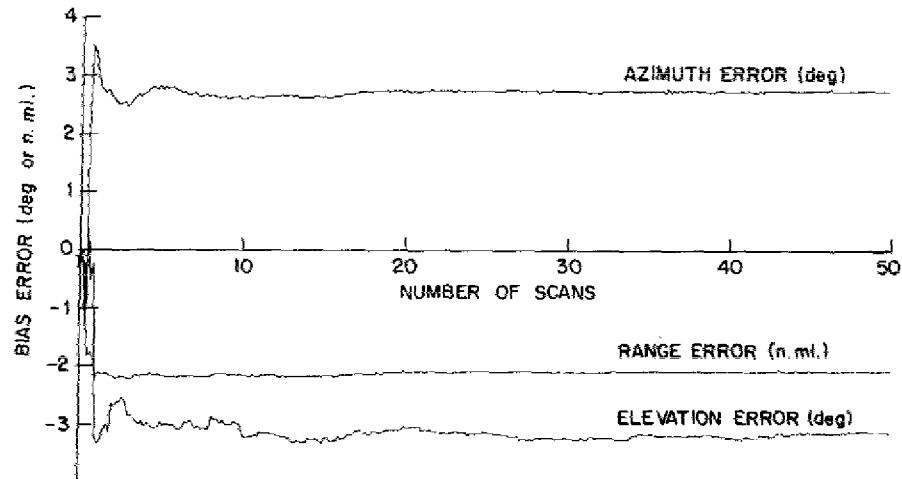


Fig. 4 — Estimate of induced bias errors in NRL radar

From the preceding results it appears that bias errors can be routinely determined when several targets are dispersed about a pair of widely separated (35 n.mi) radars. However it must be remembered that this represents an idealized situation in which the targets are stationary and evenly distributed (see Fig. 2). Because of this consideration and the availability of real data, collected by both sites on targets of opportunity, further testing of the algorithm was carried out.

4.0 RESULTS WITH REAL DATA

During September 1979, the SPS-39 radars at NRL and APL were used to simultaneously record detection data on targets of opportunity. Subsequently, these data were processed by APL to identify tracks and develop track histories from each radar's detections and to correlate tracks of common targets. APL also utilized their tracking algorithm to predict the position of all tracks at the time of north crossing of the APL radar; i.e., regardless of when detections were made an estimate of the positions of all targets was made corresponding to the time at which the APL radar had most recently swept by true north. The estimated position of each track at that time was given in rectangular Cartesian coordinates centered at each site and it was in this form that the data were made available to NRL. Fortunately the data in this form were amenable to the algorithm described in Sec. 2.0. All that was required to make it directly applicable was the transformation of the NRL tracks from the NRL coordinate system to the APL coordinate system. For each scan of the APL radar each correlated track was examined to see if both radars had detected the track since the previous north crossing. If this proved to be true the difference vector (see Eq. (4)) of the predicted positions was used as the input to the bias removal algorithm. For the data that were used this could mean as many as 15 updates by the Kalman filter in a single scan.

The effect of applying the algorithm to a specific track can be seen by examining Figs. 5 and 6. Figure 5 is a plot of the tracks developed by both radars for a common target. The tracks are displayed in the horizontal plane with APL being located at the origin and NRL/CBD located approximately 35 n.mi to the southeast of APL. The target is approaching APL from the east. The result of correcting the tracks by amounts equal to the estimated bias errors is shown in Fig. 6. In this case the start of the track was coincident with the start of the bias error estimation process; consequently initial estimates of the bias errors were applied at the beginning of the tracks. The estimated values from both radars that were used to correct the tracks are also plotted in Fig. 6; however, using the initial values of the bias errors to correct the tracks may not be representative of a working system. A conceptual system would probably have a fully developed set of bias errors available for correcting the tracks or more likely the

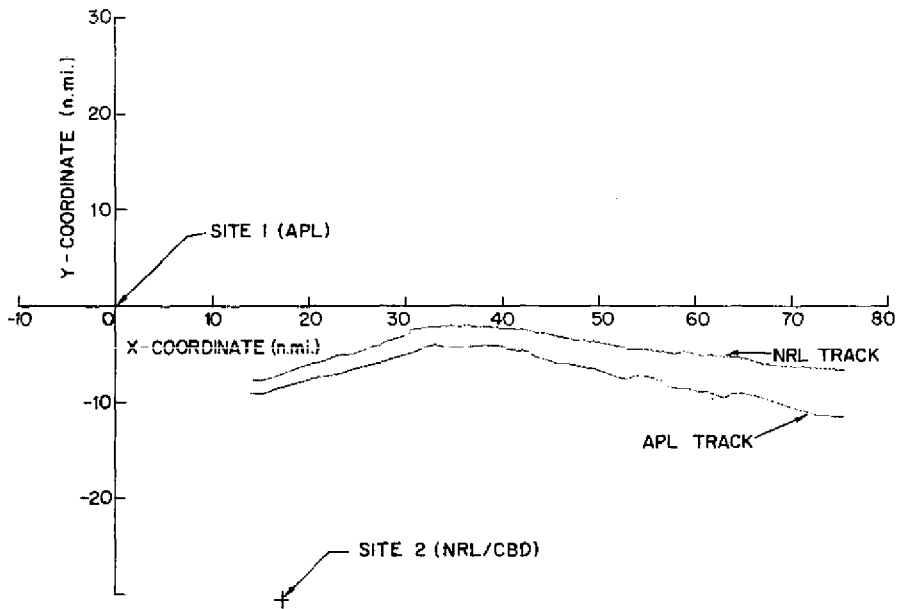


Fig. 5 - Uncorrected tracks of common target

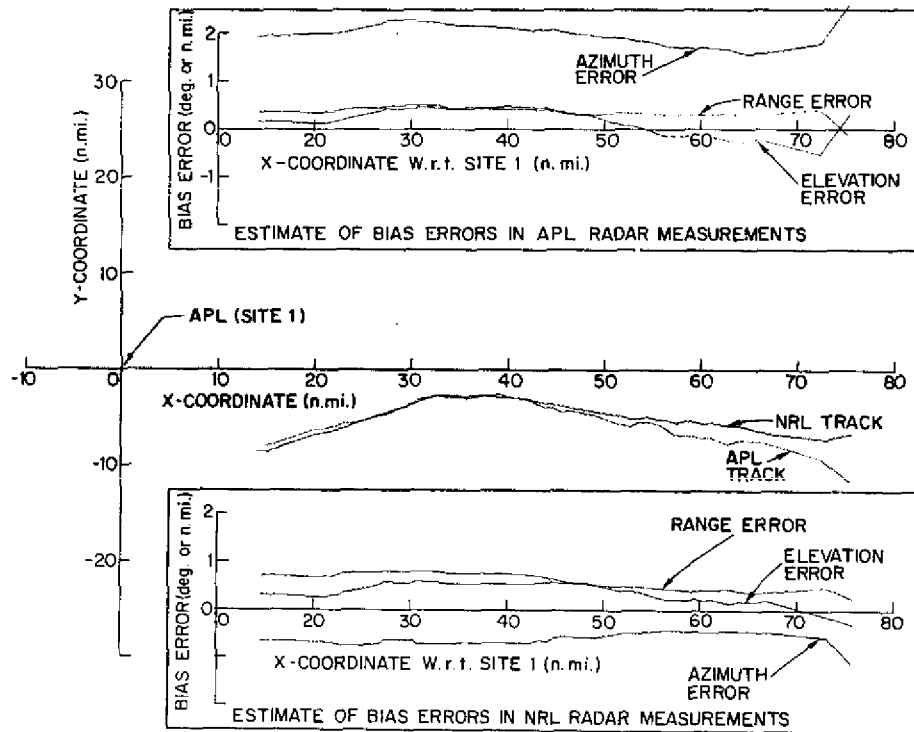


Fig. 6 - Track of common target by APL and NRL radars

raw data and updated estimates of the errors would be made on a periodic basis. To assess the effects of using a fully developed set of bias errors the track data were processed for 15 min, using the algorithm, and the following set of bias errors was obtained:

on the APL radar	0.224 n.mi in range
	2.033° in azimuth
	0.119° in elevation
on the NRL radar	0.416 n.mi in range
	-0.691° in azimuth
	0.505° in elevation.

These errors were applied to the tracks of the target shown in Fig. 5, and the results are shown in Fig. 7. Again the results are quite dramatic, and a significant improvement over Fig. 6 can be seen in the early stages of the track. Undoubtedly if such information were available to make corrections, it would simplify the correlation process and greatly reduce the number of false tracks in a multisite sensor correlation system.

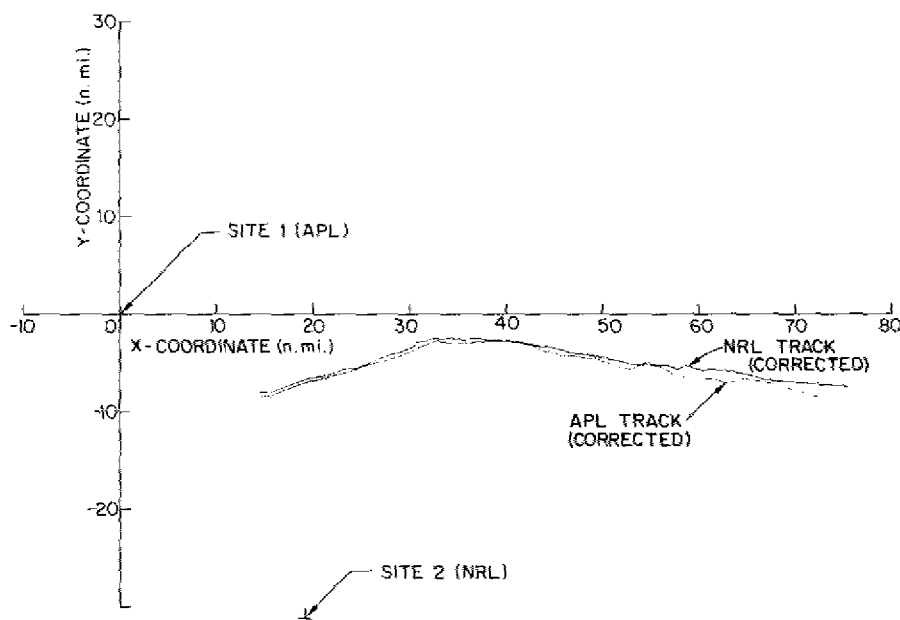


Fig. 7 — Tracks corrected with fully developed bias errors

To further validate the algorithm it was decided to apply the technique to a target in another quadrant, and a target was selected from the southwest quadrant. The target started at a point approximately 40 n.mi west and 60 n.mi south of the APL site. Initially it was headed toward the NRL site but near the end of its flight it veered toward the APL site. The two tracks of the target are plotted in Fig. 8, and the corrected tracks using the fully developed bias errors are plotted in Fig. 9. The results show a significant improvement particularly in the last half of the flight but are not as dramatic as the previous results (Fig. 7).

5.0 SUMMARY

An algorithm has been developed which can be used to detect and remove bias errors from radar measurements when the measurements are made at two separate and stationary radar sites. The algorithm has demonstrated its ability to detect bias errors and use this information to converge tracks from independent radars. This was accomplished with both real and simulated data. Since bias errors in

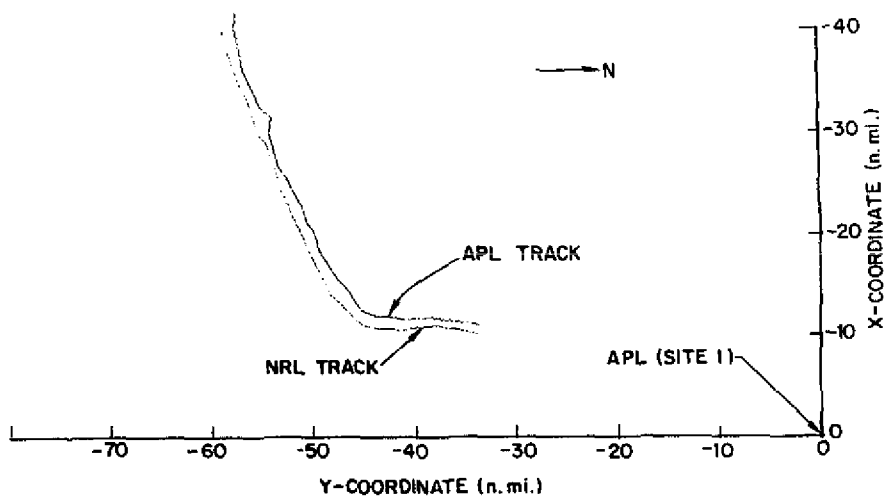


Fig. 8 - Uncorrected tracks of common target

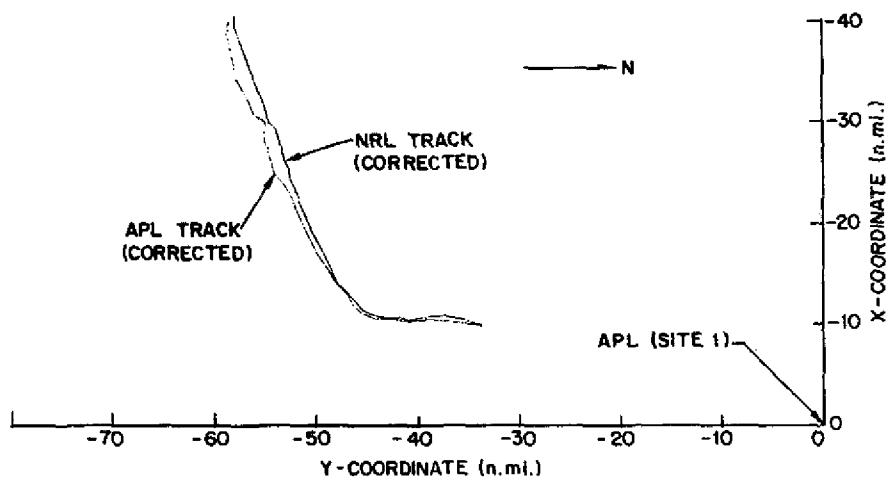


Fig. 9 - Corrected tracks of common target

radars are the rule rather than the exception, further investigation is essential if multiple platform sensor integration is to be achieved.

6.0 ACKNOWLEDGMENTS

The author wishes to thank the personnel at APL for their effort in collecting, processing, and documenting the data, and the personnel of Code 5340 (NRL) for their effort at CBD. The author also wishes to thank Dr. B. H. Cantrell for discussions and suggestions relating to several aspects of this report.

7.0 REFERENCES

1. A. Grindlay, "Multiple Platform Sensor Integration Model: MULSIM Computer Program," NRL Report 8358, December 1979.

2. B.H. Cantrell and A. Grindlay, "Multiple Site Radar Tracking System," Proc. IEEE 1980 International Radar Conference, April 1980, pp. 348-354.
3. B.H. Cantrell, A. Grindlay, and C.H. Dodge, "Formulation of a Platform-to-Platform Radar Integration System," NRL Memorandum Report 3404, December 1976.
4. G.V. Trunk and J.D. Wilson, "Tracking Filters for Multiple Platform Radar Integration," NRL Report 8087, December 1976.

APPENDIX

The position measurement vector, in a local Cartesian coordinate system, can be approximated by a linearized form as follows:

$$\begin{bmatrix} x \\ y \\ z \end{bmatrix}_2 = \begin{bmatrix} \bar{x} \\ \bar{y} \\ \bar{z} \end{bmatrix} + \begin{bmatrix} \partial x/\partial r & \partial x/\partial \eta & \partial x/\partial \alpha \\ \partial y/\partial r & \partial y/\partial \eta & \partial y/\partial \alpha \\ \partial z/\partial r & \partial z/\partial \eta & \partial z/\partial \alpha \end{bmatrix} \begin{bmatrix} \Delta R + N_r \\ \Delta \eta + N_\eta \\ \Delta \alpha + N_\alpha \end{bmatrix}_1 \quad (\text{A1})$$

where

- $(x, y, z)_2$ is the target position vector with respect to Site 1 as determined by measurements made at Site 2
- $(\bar{x}, \bar{y}, \bar{z})$ is the mean or true position vector of the target with respect to Site 1
- $(\partial x/\partial r, \partial y/\partial \eta \text{ etc.})$ are the partial derivatives of the components of the position vector with respect to changes in the measurements made at Site 2
- (r, η, α) represent the range, elevation, and azimuth measurements made at Site 2
- $(\Delta R, \Delta \eta, \Delta \alpha)_2$ represent bias errors in the measurements made at Site 2
- (N_r, N_η, N_α) represents noise in each of the measurements made at Site 2.

In vector-matrix notation Eq. (A1) can be expressed as

$$X_2 = \bar{X} + A_2(B_2 + N_2). \quad (\text{A2})$$

The elements of the A matrix are the partial derivatives of the components of the position vector. The components of the position vector are with respect to the origin located at Site 1, and the partial derivatives are taken with respect to the measurements made at Site 2. The sites are located in a latitude/longitude system in which Site 1 has the latitude/longitude pair of (θ_B, λ_B) and Site 2 has the pair (θ_A, λ_A) . The parameters δ_B, δ_A represent the height of the respective sites above the Geoid. The Cartesian coordinates of the target with respect to an origin located at Site 1 are given by:

$$\begin{bmatrix} x_1 \\ y_1 \\ z_1 \end{bmatrix} = T_c \begin{bmatrix} x_2 \\ y_2 \\ z_2 \end{bmatrix} + U_c. \quad (\text{A3})$$

The transformation from Site 2 to Site 1 is accomplished with the rotation matrix T_c and the translation matrix U_c . They are defined as follows:

$$T_c = \begin{bmatrix} \cos(\lambda_A - \lambda_B) & -\sin\theta_A \sin(\lambda_A - \lambda_B) \\ \sin\theta_B \sin(\lambda_A - \lambda_B) & \sin\theta_A \sin\theta_B \cos(\lambda_A - \lambda_B) + \cos\theta_A \cos\theta_B \\ -\cos\theta_B \sin(\lambda_A - \lambda_B) & \cos\theta_A \sin\theta_B - \sin\theta_A \cos\theta_B \cos(\lambda_A - \lambda_B) \\ \cos\theta_A \sin(\lambda_A - \lambda_B) \\ -\cos\theta_A \sin\theta_B \cos(\lambda_A - \lambda_B) + \sin\theta_A \cos\theta_B \\ \cos\theta_A \cos\theta_B \cos(\lambda_A - \lambda_B) + \sin\theta_A \sin\theta_B \end{bmatrix} \quad (A4)$$

$$U_c = \begin{bmatrix} (a + \delta_A) \cos\theta_A \sin(\lambda_A - \lambda_B) \\ -(a + \delta_A) [\cos\theta_A \sin\theta_B \cos(\lambda_A - \lambda_B) - \sin\theta_A \cos\theta_B] \\ (a + \delta_A) [\cos\theta_A \cos\theta_B \cos(\lambda_A - \lambda_B) + \sin\theta_A \sin\theta_B] - (a + \delta_B) \end{bmatrix} \quad (A5)$$

The elements of matrix A_2 can now be derived by differentiating Eq. (A3) and recalling that

$$\begin{aligned} x_2 &= r_2 \cos\eta_2 \sin\alpha_2, \\ y_2 &= r_2 \cos\eta_2 \cos\alpha_2, \\ z_2 &= r_2 \sin\eta_2. \end{aligned} \quad (A6)$$

They are as follows:

$$\begin{aligned} \partial x_1 / \partial r_2 &= T_{11} \cos\eta_2 \sin\alpha_2 + T_{12} \cos\eta_2 \cos\alpha_2 + T_{13} \sin\eta_2 \\ \partial x_1 / \partial \eta_2 &= -T_{11} r_2 \sin\eta_2 \sin\alpha_2 - T_{12} r_2 \sin\eta_2 \cos\alpha_2 + T_{13} r_2 \cos\eta_2 \\ \partial x_1 / \partial \alpha_2 &= T_{11} r_2 \cos\eta_2 \cos\alpha_2 - T_{12} r_2 \cos\eta_2 \sin\alpha_2 \\ \partial y_1 / \partial r_2 &= T_{21} \cos\eta_2 \sin\alpha_2 + T_{22} \cos\eta_2 \cos\alpha_2 + T_{23} \sin\eta_2 \\ \partial y_1 / \partial \eta_2 &= -T_{21} r_2 \sin\eta_2 \sin\alpha_2 - T_{22} r_2 \sin\eta_2 \cos\alpha_2 + T_{23} r_2 \cos\eta_2 \\ \partial y_1 / \partial \alpha_2 &= T_{21} r_2 \cos\eta_2 \cos\alpha_2 - T_{22} r_2 \cos\eta_2 \sin\alpha_2 \\ \partial z_1 / \partial r_2 &= T_{31} \cos\eta_2 \sin\alpha_2 + T_{32} \cos\eta_2 \cos\alpha_2 + T_{33} \sin\eta_2 \\ \partial z_1 / \partial \eta_2 &= -T_{31} r_2 \sin\eta_2 \sin\alpha_2 - T_{32} r_2 \sin\eta_2 \cos\alpha_2 + T_{33} r_2 \cos\eta_2 \\ \partial z_1 / \partial \alpha_2 &= T_{31} r_2 \cos\eta_2 \cos\alpha_2 - T_{32} r_2 \cos\eta_2 \sin\alpha_2, \end{aligned} \quad (A7)$$

where T_{ij} is an element of the T_c matrix. The elements of the matrix A_1 in Eq. (1) are easily derived from the relationships

$$\begin{aligned} x_1 &= r_1 \cos\eta_1 \sin\alpha_1 \\ y_1 &= r_1 \cos\eta_1 \cos\alpha_1 \\ z_1 &= r_1 \sin\eta_1 \end{aligned} \quad (A8)$$